24th INTERNATIONAL CONGRESS ON SOUND AND VIBRATION
23–27 July 2017, London

OPTIMIZING BEAMPATTERNS FOR A CONFORMAL ARRAY MOUNTED ON AN AXISYMMETRIC BODY IN FLOW NOISE FIELD

Xue-gang Li, Ming Chen, Guo-cang Sun, Cheng-you Lei and Honggang Li

Wuhan Second Ship Design and Research Institute, Wuhan 430205, China
email: xuegang608@126.com

The physical features of the flow noise for an axisymmetric body are important for improving the performance of a conformal array mounted on the underwater platform. In this paper, the uniform geometrical theory of diffraction (UTD) is introduced to calculate the flow noise field of a water-filled axisymmetric body shell. Based on the calculation results, three kinds of beamformers are designed in the flow noise field, and the performances of these beamformers are discussed. It is shown that the correlation between the flow noises received by the hydrophones mounted on the curved surface is stronger than that received by the hydrophones mounted on the head plane at the designed center frequency. Meanwhile, the signals received by the hydrophones show significant differences when the incoming signals are incidence from different directions. The scattering effects of the baffle are roughly equivalent to enlarge the aperture of the conformal array. Furthermore, the Second-Order Cone Programming beamformer in the flow noise field provides the optimal tradeoff between the sidelobe level, robustness, beamwidth and the array gain.

Keywords: flow noise, UTD, conformal array, array manifold

1. Introduction

With the development of the stealth technology, the performance of sonar mounted on an underwater platform is affected increasingly and prominently by the self-noise of the underwater vehicle. Detecting the quiet targets in the water requires improving the performance of the beamformer in the underwater systems, including the array gain, the system robustness, the sidelobe level and the mianlobe width, and so on. The flow noise is the main hydrodynamic noise at high speed. It covers the radiated noise of a target in far field as well as limiting the performance of the sonar mounted on an underwater platform. Researches [1-2] have shown that the flow noise received by the sonar of an axisymmetric body mainly come from the transition region. Due to the obstruction of the body, the performance of the sonar is mainly affected by the diffracted sound field from the transition region. Thus, it is necessary to study the diffracted sound field of the flow noise and to find a way to reduce and suppress it. Meanwhile, how to make full use of the noise correlation in the acoustic array signal processing is also valuable to study.

Recently, several methods have been introduced to calculate the flow noise. Li[3-5] studied the power spectrum and the correlation of the flow noise for an axisymmetric body by using a numerical method. However, this method is limited by the calculation scale and would take a long time for the iteration process of the flow noise to converge. In the past few years, several methods have been developed to calculate the structure near-field and the surface sound field, including the boundary element method, the Summerfeld-Watson transformation method and the transmission matrix (T-matrix) method. As for the boundary element method, it's hard to calculate the high-frequency sound field due to the limit of the calculation scale. The calculation process of the Summerfeld-

Watson transformation (SWT) method is too complicated to be practically applied. The T-matrix method is applied for wider frequency range, but it cannot be used to calculate structures with big length-width ratios. The uniform geometrical theory of diffraction (UTD) is a high frequency asymptotic method, which is suitable for calculate scattering acoustic field at high frequency. A comparison between the characteristics of different methods is shown in Table 1.

The central objective of this paper is to apply UTD method to scatter from a water-filler axisymmetric body shell. In order to give a comprehensive understanding of the scattering mechanism of the water-filler axisymmetric body shell, the scattering effect of the baffle and the array manifold are discussed. Based on the diffracted sound field calculation results, the correlation between the flow noises received by a conformal array mounted on the axisymmetric body underwater is discussed, and three kinds of beamformer are designed in the flow noise field, of which the performances of the beamforming are analyzed.

Table 1: A comparison between the characteristics of different methods

Method	Application scope	Characteristics
BEM	low frequency range	limited by calculation scale
SWT	frequency domain and wave-number frequency	high complexity
T-Matrix	broad band frequency	not suitable for structures with big length-width ratio
UTD	high frequency range	clear concept in physics, easily using and concise

2. Calculation of flow noise

The uniform geometrical theory of diffraction was first developed by Kouyoumjian and Pathak[7] and is widely used in the field of aero acoustics or electromagnetic scattering computation. It is now widely applied in engineering projects. [8-12] However, it is seldom applied in underwater acoustics. In this paper, the UTD is introduced to calculate the correlation between the flow noises received by a conformal array mounted on an axisymmetric body to overcome the complexity problems of the conventional methods.

2.1 The Uniform Geometrical theory of diffraction

According to the uniform geometrical theory of diffraction, the asymptotic solution for the pressure field Q on the surface due to the point source Q' is given by[12]

$$dp(Q\,|\,Q') = \frac{-jk\rho cu(s)}{4\pi}\left\{2\left[1-\frac{j}{kr}\right]V(\xi)\right\}DG(kr)ds\,. \tag{1}$$

where Q' and Q denote the source and the field points, respectively, as shown in Fig.1, r refers to the length of the surface ray path between the source and the observation points, k refers to the wavenumber of the exterior medium (which is taken to be the free space), ρ and c are the density and the sound speed of the medium, respectively, and $u(s)$ is the vibration velocity of the infinitesimal source ds.

The function $V(\xi)$ in Eq.(1) is the hard surface Fock integral and is given by

$$V(\xi) = \frac{\xi^{\frac{1}{2}}e^{j\frac{\pi}{4}}}{2\sqrt{\pi}}\int_{\infty e^{-j2\pi/3}}^{\infty}\frac{W_2(\tau)}{W_2'(\tau)}e^{-j\xi\tau}d\tau\,. \tag{2}$$

where $W_2(\tau)$ denotes the Fock-type Airy function defined by

$$W_2(\tau) = \frac{1}{\sqrt{\pi}} \int_{\infty e^{-j2\pi/3}}^{\infty} e^{\tau Z - Z^3/3} dZ \,. \tag{3}$$

and $W_2'(\tau)$ denotes the derivative of $W_2(\tau)$ with respect to τ. The ξ is the generalized Fock parameter for the arbitrary convex surface, and is defined by

$$\xi = \left(\frac{k}{2}\right)^{\frac{1}{3}} \int_{Q'}^{Q} \frac{1}{\left[\rho_g(r)\right]^{\frac{2}{3}}} dr \,. \tag{4}$$

which is the arc length normalized by the wavenumber k and the radius of the curvature $\rho_g(r)$. Note that ξ =0 defines the lit region, ξ<1 defines the penumbra region, and ξ >>1 defines the deep shadow. Our solution is valid for all $\xi \geq 0$. The $G(kr)$ in Eq.(1) is the Green function in the free field, and is given by

$$G(kr) = \frac{e^{-jkr}}{r} \,. \tag{5}$$

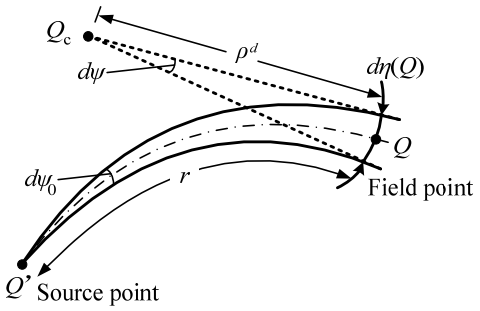

Figure 1: Surface ray strip.

The surface ray divergence factor D is given by

$$D = \sqrt{\frac{r d\psi_0}{d\eta(Q)}} = \sqrt{\frac{r d\psi_0}{\rho^d d\psi}} \,. \tag{6}$$

In Fig.1, a pair of infinitesimally separated surface rays adjacent to the central ray from Q to $Q'$are shown. These adjacent rays constitute a surface strip, and the $d\psi_0$ in Eq.(5) refers to the angle between these adjacent surface rays at the source point Q'. The $d\psi$ is the angle between the backward tangents of the same pair of adjacent surface rays at the point Q. The tangents cross at point Q_c. The ρ^d is the distance between points Q and Q_c. The $d\eta(Q)$ denotes the width of the surface ray strip at the point Q. According to the generalized Fermat's principle, rays are shed or diffracted from the surface ray along the forward tangents of the geodesic surface ray path. Hence, energy is continuously lost from the surface ray field due to rays shed or diffracted from the surface ray.

The asymptotic solution for the pressure field Q can be calculated by adding the entire infinitesimal sources on the surface. Assuming that S is the vibration area on the surface, the total pressure in the field point Q caused by the vibration area S can be written as

$$\overline{p}(Q \mid S) = \int_S \frac{-jk\rho cu(s)}{4\pi} \left\{ 2\left[1 - \frac{j}{kr}\right] V(\xi) \right\} DG(kr) ds \,. \tag{7}$$

2.2 Ray tracing on body surface

The surface ray paths on the head of the axisymmetric body are calculated by using the dynamic programming method. The boundary layer of an axisymmetric body is shown in Fig.2(a). The

source of flow noise under consideration locates at the transition region and the turbulent boundary layer on the axisymmetric body. It has been shown that when the frequency of the flow noise is less than 40 kHz, the flow noise received at the stagnation point of the axisymmetric body mainly comes from the transition region. [1,2] The surface ray paths calculation results are shown in Fig.3.

Figure 2: The boundary layer of an axisymmetric body.

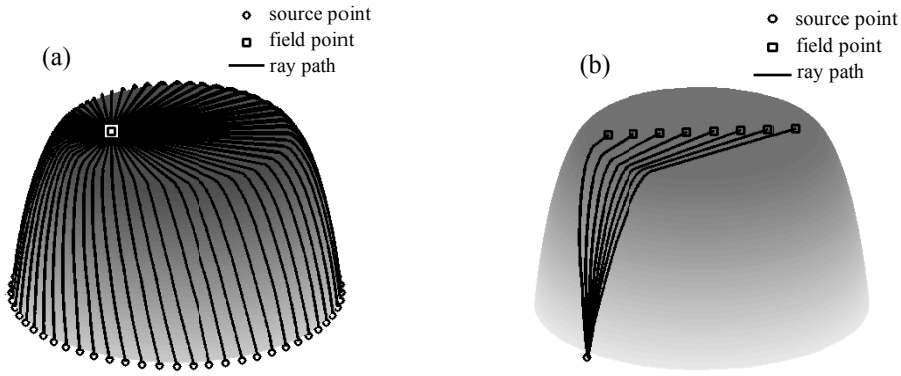

Figure 3: The ray paths on the body surface (a) from 60 source points to one receiving point, and (b) from one source point to 8 receiving points.

2.3 Correlation of the flow noise

The correlation of the flow noise from transition region of an axisymmetric body is simulated in this section. Firstly, 60 independent narrowband Gaussian noise sequences are created by the numerical method, and the center frequency is assumed to be 30 kHz. The mean value and the variance of the sequences are 0 and δ, respectively. The simplified model of the conformal array is shown in Fig.4. The designed center frequency is 30 kHz based on the array configuration method of half-wavelength. The serial numbers of the hydrophones in the black box are 1#, 2# … 16# from left to right, respectively.

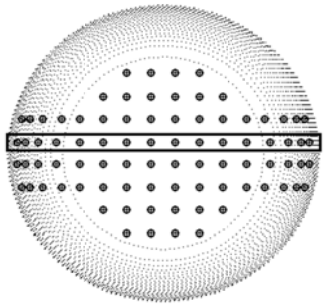

Figure 4: Conformal array on the head of the axisymmetric body.

Assuming that the phase difference and the amplitude variation from the source point k to the ith hydrophone are φ_{ki} and A_{ki}, respectively, then the noise sequence received in the ith hydrophone can be written as

$$x_i = \sum_{k=1}^{60} n_k \cdot A_{ki} e^{-j\varphi_{ki}} . \tag{8}$$

For any two hydrophones *i* and *j*, the correlation coefficient of the flow noise is given by

$$\rho_{ij} = \frac{E(x_i x_j^*)}{\sqrt{\mathrm{var}(x_i) \cdot \mathrm{var}(x_j)}}, \tag{9}$$

where *E* and the superscript * denote the mean value and the conjugate, respectively. And var means variance.

The correlations of the 16 hydrophones in the black box are shown in Fig.5. The center frequencies of the flow noise in Figs.5(a) and 5(b) are 15kHz and 30kHz, respectively. The bandwidth of the flow noise is 1 kHz. It can be seen that the correlations of the hydrophones on the curved surface are stronger than that on the head plane at the designed center frequency. The physical reason is that the flow noises to the hydrophones on the curved surface mainly come from the point sources that are close to these hydrophones. And the flow noises of the hydrophones on the head plane come from all point sources.

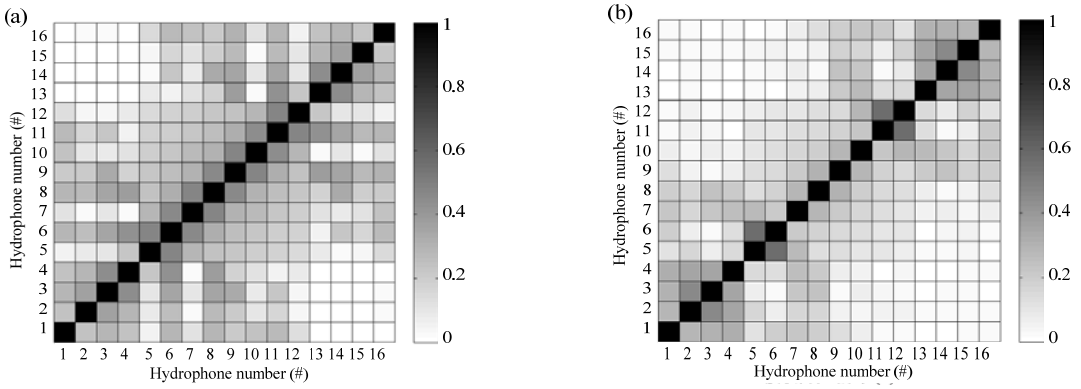

Figure 5: The noise correlation in black box with center frequency at (a)15 kHz and (b) 30 kHz.

3. Beamforming in flow noise field

3.1 Calculation of array manifold

In many engineering applications, the key problem in the beam pattern design and optimization of sensor arrays is to obtain array manifold. For an array consisting of omni-directional hydrophones, the array manifold is determined by the geometric relationships of the hydrophones. However, the directivities of the hydrophones mounted on an axisymmetric body are significantly influenced by the scattering effect of the array baffle. The boundary element methods are widely used to calculate the scattering field. The boundary element model of the axisymmetric body is shown in Fig.6. In order to improve the accuracy of solutions, meshes are refined around the hydrophones. The black dots denote the position of the hydrophones. The serial numbers of the hydrophones are 1#, 2# … 16# from left to right, respectively. The incoming signals satisfy the far field condition and plane wave condition. The signal frequency is set at 30 kHz corresponding to the array configuration method of half-wavelength. The responses of the hydrophones to the incoming signals are calculated from directions -90° to 90° by a step value of 1°. Then the array manifold can be obtained by combining the response vector.

The responses of the hydrophones to the incoming signal from different directions are calculated by the boundary element method. The directivities of the hydrophones with serial number 1#, 3# and 8# are shown in Fig.7 (a), (b) and (c), respectively. It is noted that $\theta = 0°$ correspond to the direction perpendicular to head surface of the axisymmetric body in Fig.6. It can be seen that the responses of the hydrophones to the incoming signal from different directions show significant differ-

ences. Therefore, the responses of the hydrophones mounted on the axisymmetric body cannot be assumed to be omni-directional.

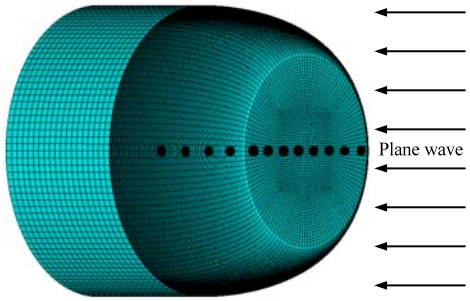

Figure 6: The boundary element model of the axisymmetric body.

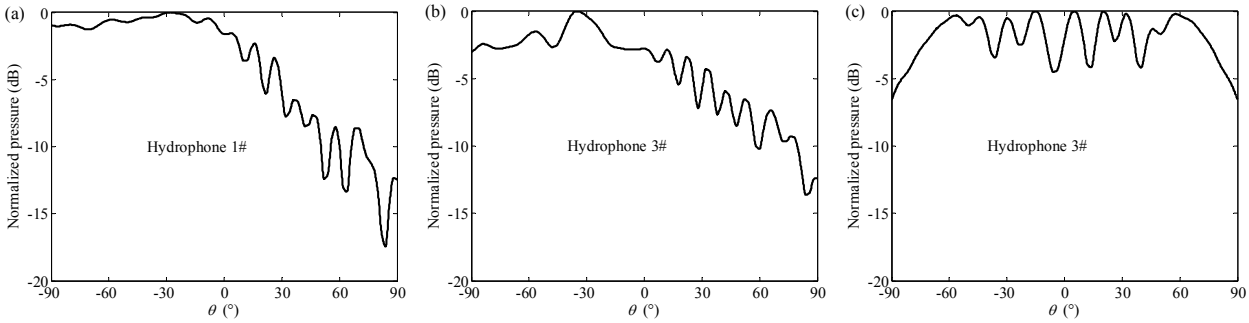

Figure 7: The directivities of the hydrophones with serial number (a) 1#, (b) 3# and (c) 8#.

3.2 Beamforming in flow noise field

Once we have gotten the array manifold, the beampatterns can be obtained by using different beamforming methods. The beampatterns formed by the conventional beamforming (CBF)[13] method are shown in Fig.8(a). The main lobes are set to point to the direction of 0°. It can be seen that the side lobes of the beampattern considering baffle effects are significantly lower than the ones neglecting baffle effects. The solid line and the dashed line in Fig.8(b) shows the array gains (AG) versus azimuth angle for considering baffle effects and neglecting baffle effects, respectively. It can be seen that the maximum values of the AG correspond to the direction of 0°. Moreover, the AG for considering baffle effects is about 2 ~ 5 dB higher than that for neglecting baffle effects. In fact, the scattering effects of the baffle are roughly equivalent to enlarge the aperture of the conformal array. So the beampatterns have lower sidelobes and higher AG when considering baffle effects.

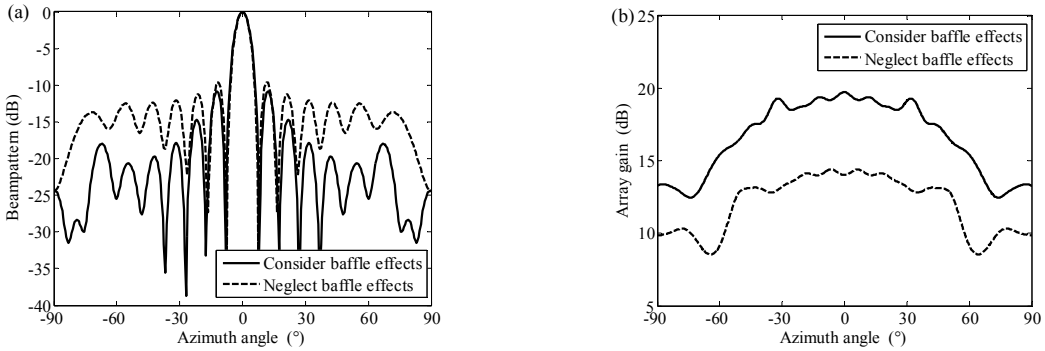

Figure 8: The (a) beampatterns and (b) array gains of the CBF.

The correlations of the flow noise in Section 2.3 and the array manifold obtained in Section 3.1 are used to design different beamformers. In this paper, the beampatterns are formed by three different methods, which are the CBF, the Minimum Variance Distortionless Response (MVDR) beamforming and the SOCP beamforming. Figure 9 (a), (b) and (c) correspond to the main lobes pointing to the direction of 0°, -20° and -45°, respectively. The desired sidelobe levels of the SOCP beamforming are set to be -15 dB. It can be seen that the beampattern formed by the MVDR meth-

od has the highest sidelobe level and a relatively narrower beamwidth. The beampatterns formed by the SOCP method has the most optimal sidelobe level (constant sidelobe level) and a relatively wider beamwidth. The beampatterns formed by the CBF has a moderate sidelobe level and beamwidth. It should be noted that the beamwidth of the SOCP beamformer would be narrower when setting a relatively higher sidelobe level.

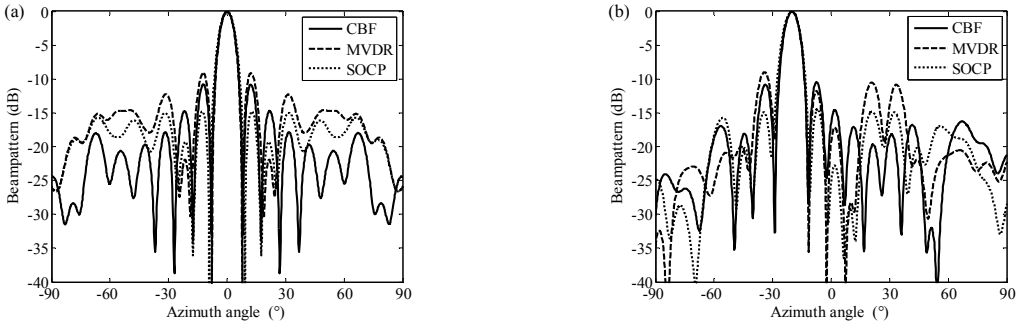

Figure 9: The beampatterns with the main lobes pointing to the direction of (a) 0°and(b) -20°.

Figure.10(a) shows the array gains versus azimuth angle for the CBF, MVDR and SOCP beamformers. The array gains are calculated in the flow noise field. It can be seen that the MVDR beamformer has the highest array gains. The SOCP beamformer has a relatively lower array gain compared with the MVDR beamformer. The CBF beamformer has the lowest array gains. The white noise gain is calculated in the white noise field and represents the robustness of a beamformer. Fig.10(b) shows the white noise gains versus azimuth angle for the CBF, MVDR and SOCP beamformers. It can be seen that the CBF beamformer has the best robustness. The MVDR beamformer has the worst robustness. The SOCP beamformer has a moderate robustness. According to the analysis above, it can be concluded that the SOCP beamformer provides the optimal tradeoff among the sidelobe level, robustness, beamwidth and the array gain.

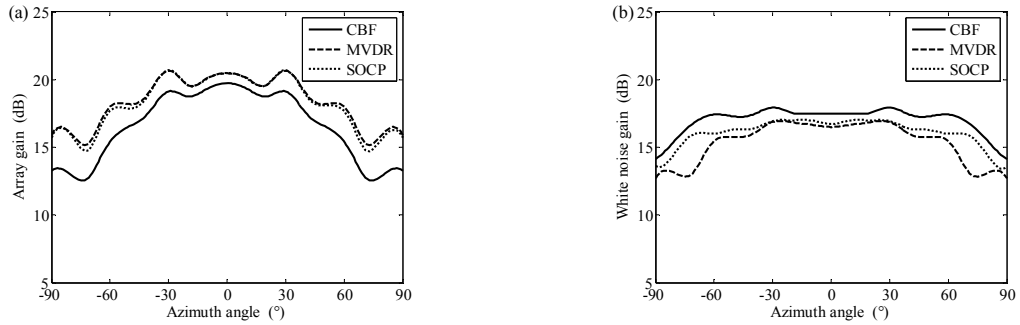

Figure 10: The (a)array gains and the (b)white noise gains versus azimuth angle.

4. Conclusions

The correlations of the flow noise for an axisymmetric body are important for improving the performance of the conformal array mounted on the underwater platform.

The uniform geometrical theory of diffraction (UTD) is introduced to calculate the correlation between the flow noises received by a conformal array to overcome the complexity problem of the conventional methods. Based on the calculation results, three kinds of beamformers are designed in the flow noise field and the performances are discussed. The array manifold is calculated by using the boundary element method, and three kinds of beamformer are designed by using the correlation information of the flow noise and the array manifold considering the baffle effects. The performances of the beamforming are analyzed. The following results are obtained. The flow noise received by the acoustic array on the curved surface has relatively stronger correlation than that on the head plane at the designed center frequency. The responses of the hydrophones to the incidence signal from different directions show significant differences. The scattering effects of the baffle are

roughly equivalent to enlarge the aperture of the conformal array. The SOCP beamformer in the flow noise field provides the optimal tradeoff among the sidelobe level, robustness, beamwidth and the array gain. It should be noted that the beamwidth of the SOCP beamformer would be narrowed when setting a relatively higher sidelobe level.

Acknowledgement

This work is supported by the National Natural Science Foundation of China (Grand No. 51409199).

References

1 Lauchle G C. On the radiated noise due to boundary-layer transition. *J. Acoust. Soc. Am.*, **67**(1): 158-168, (1980).

2 Arakeri V H, Satyanarayan S G, Mani K and Sharma S D. Studies on scaling of flow noise received at the stagnation point of an axisymmetric body. *J. Sound. Vib.* **146**(3): 449-462, (1991).

3 Li X G, Yang K D and Wang Y. The diffracted sound field from the transition region of an axisymmetric body in water. *Chin. Phys. B*, **20**(7): 074301-1_9, (2011).

4 Li X G, Yang K D and Wang Y. The power spectrum and correlation of flow noise for an axisymmetric body in water. *Chin. Phys. B*, **20**(6): 064302-1_8, (2011).

5 Li X G, Yang K D and Ma Y L. Flow noise calculation using the mutual coupling between vulcanized rubber and the flow around in water. *Chin. Phys. Lett.*, **29**(6): 064301-1_3, (2012).

6 Levy B R and Keller J B, Diffraction by a smooth object. *Communications on pure and applied mathematics* **12**(1): 159-209, (1959).

7 Kouyoumjian R G and Pathak P H, A uniform geometrical theory of diffraction for an edge in a perfectly conducting surface. *Proceeding of the IEEE* **62**(11): 1448-1461, (1974).

8 Rousseau P R and Pathak P H, Time-domain uniform geometrical theory of diffraction for a curved wedge. *Antennas and Propagation, IEEE Transactions on* **43**(12):1375-1382, (1995).

9 Holm P D, UTD-diffraction coefficients for higher order wedge diffracted fields. *Antennas and Propagation, IEEE Transactions on* **44**(6):879-888, (1996).

10 Volakis J, A uniform geometrical theory of diffraction for an imperfectly conducting half-plane. *Antennas and Propagation, IEEE Transactions on* **34**(2):172-180, (1986).

11 Veruttipong T W, Time domain version of the uniform GTD. *Antennas and Propagation, IEEE Transactions on* **38**(11): 1757-1764, (1990).

12 Pathak P H and Wang N, Ray analysis of mutual coupling between antennas on a convex surface. *Antennas and Propagation, IEEE Transactions on* **29**(6)(1981) 911-922.

13 Yan S F and Ma Y L. Robust super gain beamforming for circular array via second-order cone programming. *Applied Acoustics*, **66**(9): 1018-1032, (2005).